IOSR Journal of Mechanical and Civil Engineering (IOSR-JMCE)
e-ISSN: 2278-1684, p-ISSN: 2320-334X, Volume 22, Issue 2 Ser. 1 (Mar. – Apr. 2025), PP 15-22
www.iosrjournals.org

Numerical Observation Of Aerodynamic Characteristics Of A Biconvex Airfoil At Supersonic Flow

Deboprio Biswas[1], Rubiat Mustak[2, *], Smaran Bakchi[3]
[1,2,3] *Department Of Mechanical Engineering, Khulna University Of Engineering & Technology, Khulna -9203, Bangladesh.*

Abstract
This study focuses on the observation of aerodynamic characteristics of a biconvex airfoil at high Mach number flow or supersonic flow. To understand the influence of supersonic flow on the aerodynamic characteristics of a biconvex airfoil numerical simulation was done using ANSYS Fluent. For the simulation purpose a two-dimensional, turbulent, steady flow is considered. The simulation was done with appropriate flow domain and boundary conditions. A C-type flow domain is considered. SST k-ω viscous model is used to predict the flow turbulence. The simulation was done for Mach number 1.7. With the help of existing literature validation was done. Mesh independency test was also done. Flow visualization is done to view the shock waves and expansion waves clearly and properly. The outcomes reveal that with the increase of angle of attack the airfoil's coefficient of lift increases until stall occurred. The stall occurred at an angle of attack 30° with a drastic loss of lift coefficient. The coefficient of drag also increases with the increase of angle of attack. The lift to drag ratio increases until 6° angle of attack than it falls. The biconvex airfoil shows maximum aerodynamic efficiency at 6° angle of attack.

KeyWords: *Biconvex Airfoil, Mach Number, Supersonic Flow, Aerodynamic Characteristics, CFD Simulation.*

Date of Submission: 07-02-2025 Date of Acceptance: 02-03-2025

I. Introduction

After the invention of first aircraft, men are continuously trying to improve the technical features of the airplanes. The old-fashioned aircraft now turns into a fighter jet. Now a day's aircrafts are flying at a speed faster than sound. These supersonic air vehicles require specialized wing design to maintain its flight. The cross section of an airplane's wing is termed as airfoil [1,2]. Biconvex airfoil, which is created by connecting two circular arcs, is more frequently used for supersonic aircrafts [3]. Researchers are continuously trying to improve the aerodynamic characteristics of this biconvex airfoil. A biconvex airfoil with a slightly curved leading edge was examined by Benadict et al. Both supersonic and hypersonic speeds of the airfoil were investigated. The outcomes showed that lift and drag coefficient decreased as Mach no increased. As increasing Mach no 2 to 7 lift coefficient decreased by 69.7% and the drag coefficient decreased by 49.3% respectively. Since drag coefficient decreased, it was concluded that biconvex airfoil can be used for hypersonic speed as well as supersonic speed [4]. Kinaci studied supersonic flow over a double circular airfoil at different radii. Gridgen V15 which is a mesh creation application was used to build the airfoil and Star-CCM+ was used for the numerical simulations. It is observed that drag coefficient for analytical and numerical simulation was 0.02371 and 0.0329 respectively. The difference between the drag coefficient was 27.93% between analytical and numerical results [5]. Shivaji et al. used a biconvex airfoil to study the Supersonic Natural Laminar Flow (SNLF) phenomenon on a wing. The research focused on understanding the characteristics of thin airfoils at supersonic speeds, particularly in the context of designing wings for Supersonic Business Jets (SBJs). Difference between lift and drag coefficients for the calculated and simulated results are 2.69% and 9.9%. The outcomes settled that supersonic linearized theory provides satisfactory agreement for analyzing thin airfoils, with the temperature and pressure ranges falling within acceptable levels [6]. Tulitia et al. studied drag reduction and buffeting alleviation in transonic periodic flow over biconvex airfoils. Flow control techniques, and surface cooling concepts for 14% and 18% thickness biconvex airfoil in transonic periodic flow were investigated. It is found that positive cooling and bump have a positive impact on buffeting alleviation and drag reduction [7]. Lewis et al. performed numerical simulation on steady supersonic viscous flow. For steady flow, a noniterative, space marching, finite-difference method was created. The results showed that the devised technique can be used for supersonic viscous flow over arbitrary shaped bodies in a steady state. The numerical algorithm's calculated findings correspond well with those from more expensive time marching methods [8].Weichen et al. numerically investigated compressible flow past an aerofoil. A 18% thick circular -arc airfoil with detached eddy model was used. The Reynolds number was $1.1*10^7$ and the free stream Mach number was 0.76. The study

examined coherent structure kinematics, turbulent boundary layer properties, moving shock wave behaviors, and flow evolution in dynamic processes. A feedback model that can forecast shock wave self-sustaining motions was created. Based on the characteristics of a moving shock wave, three common flow regimes were displayed. These include the turbulent boundary layer's interaction, the intermittent boundary layer's separation, and the connected boundary layer [9]. Khalid et al. simulated 2D inviscid supersonic flow using the McCormack's predictor-corrector scheme. The results were verified with results from classical theories and CFD package. It is found that, the numerical solutions without involvement of numerical dissipation are discontinuous. Numerical dissipation was applied to remove that discontinuity. It is also found that selecting courant number is more important than grid spacing [10]. The shear stress transport turbulent model was utilized by Sarkar et al. to numerically assess the critical angle of attack, lift to drag ratio, stall area, pressure distribution, velocity distribution, and other aerodynamic forces over the airfoil model at a high Reynolds number [11].

From the above discussion it is clear that, biconvex airfoils are studied in various conditions to understand its behaviors or characteristics properly during flights. A lot of conditions or combinations have already been applied. This study observes the aerodynamic characteristics of a biconvex airfoil at a unique Mach number that has not been explored previously. The Mach number which is taken for the current study is not studied yet.

II. Methodology

Continuity, momentum and energy equations are the fundamental governing equations utilized by ANSYS Fluent to perform the simulations quickly and accurately [12]. These governing equations can be written as,

$$\frac{\delta(\rho a)}{\delta x} + \frac{\delta(\rho b)}{\delta y} = 0 \quad (1)$$

$$a\frac{\partial(\rho a)}{\partial x} + b\frac{\partial(\rho a)}{\partial y} = -\frac{\partial P}{\partial x} + \frac{\partial \tau_{xx}}{\partial x} + \frac{\partial \tau_{yx}}{\partial y} \quad (2)$$

$$a\frac{\partial(\rho b)}{\partial x} + b\frac{\partial(\rho b)}{\partial y} = -\frac{\partial P}{\partial y} + \frac{\partial \tau_{xy}}{\partial x} + \frac{\partial \tau_{yy}}{\partial y} \quad (3)$$

$$\rho c_v \frac{dT}{dt} = k\nabla^2 + \phi \quad (4)$$

Here equation (1) is the continuity equation. The Navier-Stokes equations are represented by equation no (2) and (3). While the equation (4) expresses the energy terms. In the above-mentioned equations μ represented the viscosity, ρ is the density, p is the pressure, τ is the shear stress, while ϕ is the viscous dissipation at temperature T. The SST k-ω turbulence model is used by ANSYS Fluent to provide the best results for supersonic flow prediction [13]. Based on the recommendation of ANSYS Fluent and previous literatures, SST k-ω turbulence model is used for the current study. The steps for simulating the biconvex airfoil are described in this portion of the current article. In ANSYS Fluent, firstly geometry of the airfoil is drawn. In this project geometry is drawn in Design modeler. In top of design modeler tool, under concept section, 3D curve option is available. This helps to import the airfoil coordinates directly to the Design modeler. There is another way to creating the geometry which is used in this project. Firstly, point is created by inserting coordinate file under concept menu. After generating points, lines are formed by connecting the points. After generating lines, upper and lower wall of the airfoil is visible. Later meshing was done. After generating the mesh, various parameters needed to be checked which determines mesh quality. These parameters are found under mesh metric section. These parameters are skewness, orthogonal quality, aspect ratio etc. For the setup module firstly, solver type was selected. In Fluent, pressure and density-based solver are available. For incompressible flow, pressure-based solver is preferred. But for compressible flow, density-based solver is required. For this simulation, density-based solver is used. For one Mach no (i.e., Ma=1.7) simulation is performed. Since Mach no is larger than 0.3 compressibility effect will consider. In model section energy equation is turned on. SST k-omega turbulence model is chosen. Then in material selection section, ideal gas is selected. Its viscosity is given by Southerland law (three coefficient method). After selecting this material, it is assigned to fluid surface body. Flow, turbulent kinetic energy and specific dissipation rate all are selected second order Upwind type. In solution control menu, Courant number is provided. The length of time a particle remains in a single mesh cell is represented by the dimensionless Courant number. Next step was report definition section. Here C_l and C_d reports are defined from force report menu. Standard initialization was used and each time solution was initialized from farfield_1. Last step was to set a specific no of iteration with the convergence criteria (1*10e-04) and then running and monitoring the solution. The current study utilized a structured C-type mesh. The flow domain is, 12c apart from the airfoil profile in the grid's top and lower bounds which stretches 20c downstream to 12c upstream.

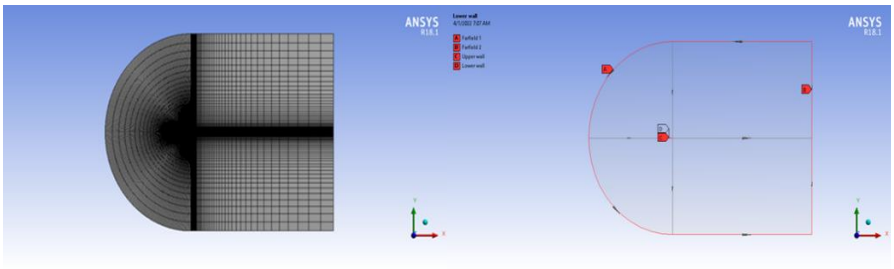

(a) **(b)**

Fig 1: (a) Meshing for the current simulation and (b) Boundary Selection.

For generating the mesh edge sizing and face meshing were applied. The generated grid has 52800 elements and 53240 nodes. In specific named selection zones, pressure far-field and pressure outlet boundary conditions are applied. While no-slip boundary condition is considered for the airfoil walls.

III. Mesh Independency & Model Validation

To identify the appropriate number of grid elements mesh independency test was done. Edge sizing was used to vary the number of elements. Coefficient of lift C_L and Coefficient of Drag C_D are considered as observing parameters to understand the influence of number of grid elements on the simulation outcomes. Table 1 shows the variation of these considering parameters.

Table no 1: Variation of different aerodynamic characteristics with number of elements.

Grid	Number of elements	Growth factor	C_L	C_D
1	28800	1.1	1.542185	0.592004
2	40000	1.1	1.547965	0.590105
3	52800	1.1	1.552700	0.592239
4	57500	1.1	1.552775	0.592211
5	62400	1.1	1.552775	0.592226

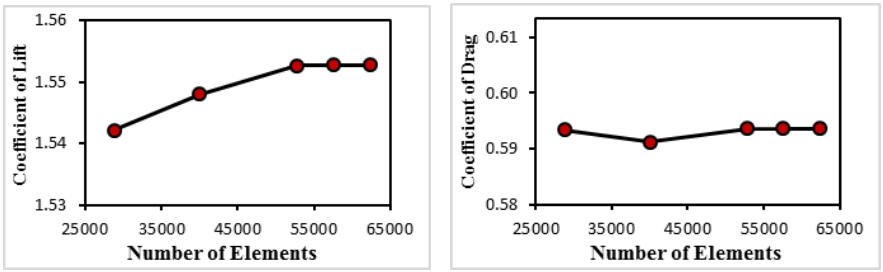

Fig 2: Variation of C_L and C_D with the number of elements.

The values of lift and drag coefficient were observed closely with the change of elements number. Table 1 and Figure 2 demonstrate that, initially with the change of elements number the values of the coefficients of lift C_L and drag C_D fluctuates. But after 52800 elements these values become stable. Further increase of elements number do not affect these parameters. As a result, in order to avoid complexity with minimum cost and time the simulation was done using 52800 elements. The current simulation setup or conditions were validated against the existing literature of Ebrahim Hosseini [14]. Values of coefficient of lift obtained from the current study were compared with the existing literature [14]. Comparison was done at a Mach number of 1.2 and up to 18° angle of attack. A good agreement was observed between the current simulation data and existing literature [14], shown by figure 3, which verified the appropriateness of the current numerical procedure.

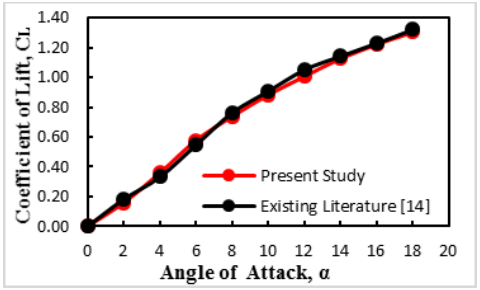

Fig 3: Comparison of C_L between present study and existing literature [14].

IV. Results And Discussion

Variation of Aerodynamic Characteristics at Mach Number 1.7

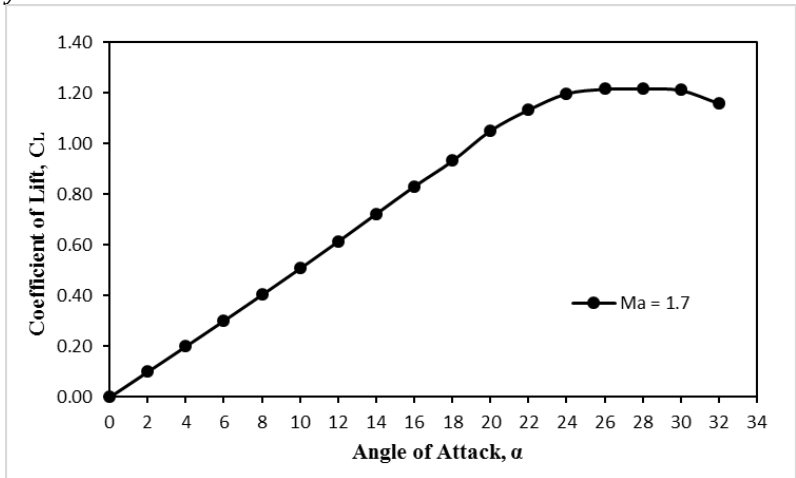

Fig 4: Changes of lift coefficient with the angle of attack.

The variation of coefficient of lift or C_L is shown by figure 4. It can be seen from figure 4, with the increase of angle of attack from 0°, the coefficient of lift starts to increase until a critical angle of attack. Until this critical angle of attack the airfoil lift generation increases with the angle of attack due the increased pressure differences between the suction and pressure side of the airfoil. At the critical angle of attack the airfoil suddenly losses lift with the drastic increment of drag due to the separation of flows. This critical angle of attack where the boundary layer separation or flow separation occurs is termed as stall angle of attack. At stall the airfoil exhibits undesired characteristics. The stall angle for the current study is 30° angle of attack at supersonic flow with a Mach number of 1.7. In another word, the biconvex airfoil subjected to flow separation with drastic loss of lift at 30° angle of attack when the Mach number is 1.7, which is a supersonic flow.

Figure 5 shows the variation of coefficient of drag or C_D with the angle of attack. Same as the lift coefficient the drag coefficient also starts to increase with the increase of angle of attack. The airfoil is subjected to more drag forces as the angle of attack starts to increase from 0°. But after the stall where flow separation occurs, the coefficient of drag is still increasing though the lift coefficient falls. The drag forces increase suddenly and abruptly after the stall condition. At stall where the flow separated from the airfoil surfaces, the drag increases due to the flow in the reverse direction.

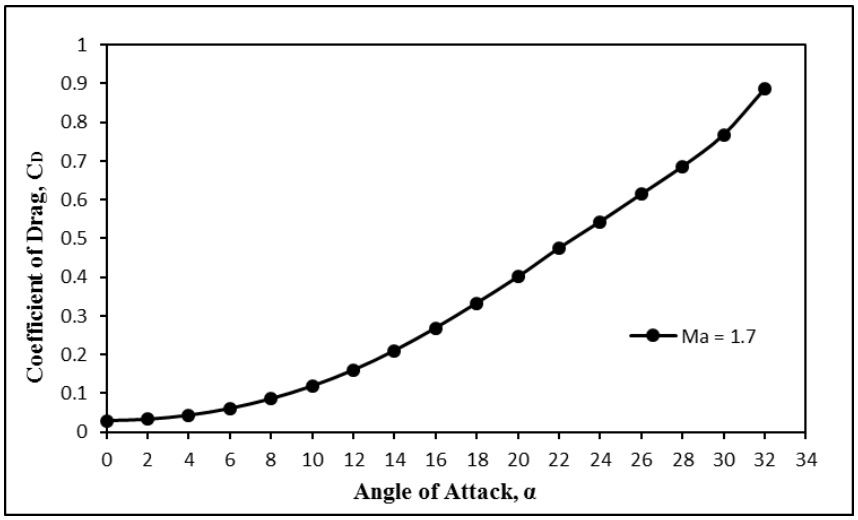

Fig 5: Drag coefficient variations with the angle of attack.

Figure 6 shows the variation of aerodynamic efficiency or the lift to drag ratio with the increase of angle of attack. The lift to drag ratio increases with the increase of angle of attack upto a certain angle of attack. At the current supersonic flow where the Mach number is 1.7, the biconvex airfoil shows maximum aerodynamic efficiency or lift to drag ratio at 6° angle of attack. After 6° angle of attack the lift to drag ratio starts to decrease.

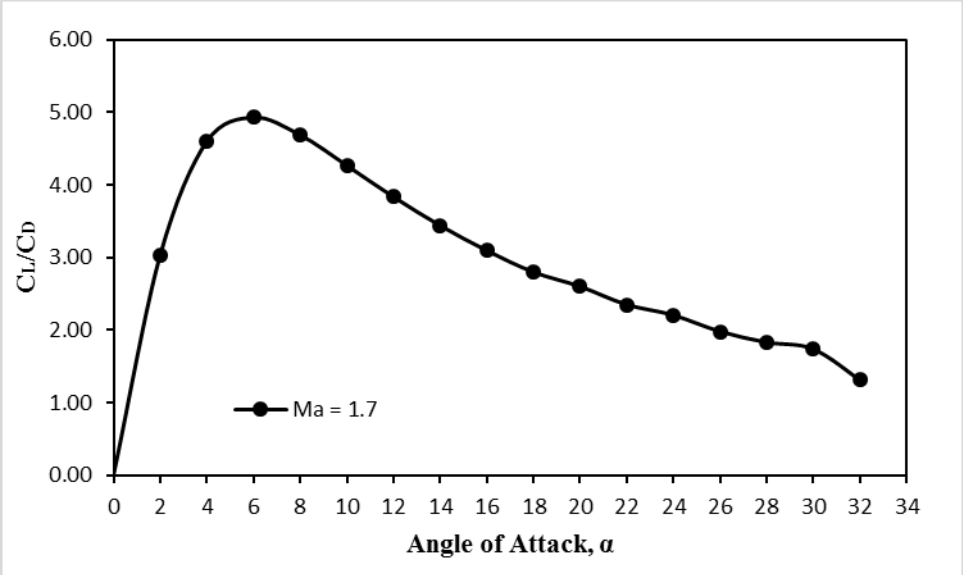

Fig 6: Changes of lift to drag ratio with the angle of attack.

Pressure Contours at Mach Number 1.7

To understand the pressure distribution around the biconvex airfoil surfaces the pressure contours are visualized. The flow visualization for the pressure distribution is shown by figure 7 and 8. Figure 7 and 8 show the variation of surface pressure with the angle of attack at supersonic flow with a Mach number of 1.7. In the visualized pressure contours, the blue color indicates the lower magnitude of surface pressure, while the green and yellow color specify the higher magnitude. From the visualization it can be seen that, pressure in the lower surface of airfoil is higher than the upper surface which enables the airfoil to generate lift. With the increase of angle of attack the shock waves and expansion waves starts to appear. With the increase of angle of attack pressure on the lower surface increases. After a certain angle of attack the flow starts to change its direction due to the adverse pressure gradient. The flow separation point moves forward with the increase of angle of attack. The zone of silence is visible between the oblique shocks on the upper surface. Bow shock wave is formed near the leading edge of the airfoil, while the oblique shock wave appears at the trailing edge of the airfoil.

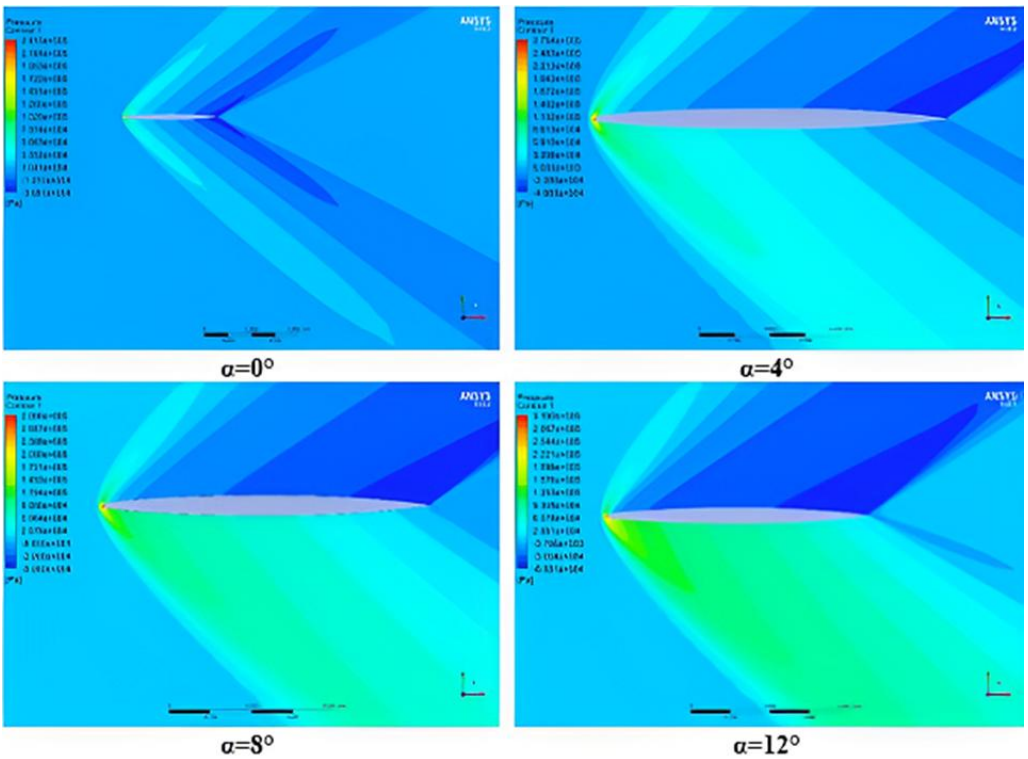

Fig 7: Pressure contours for Mach number 1.7.

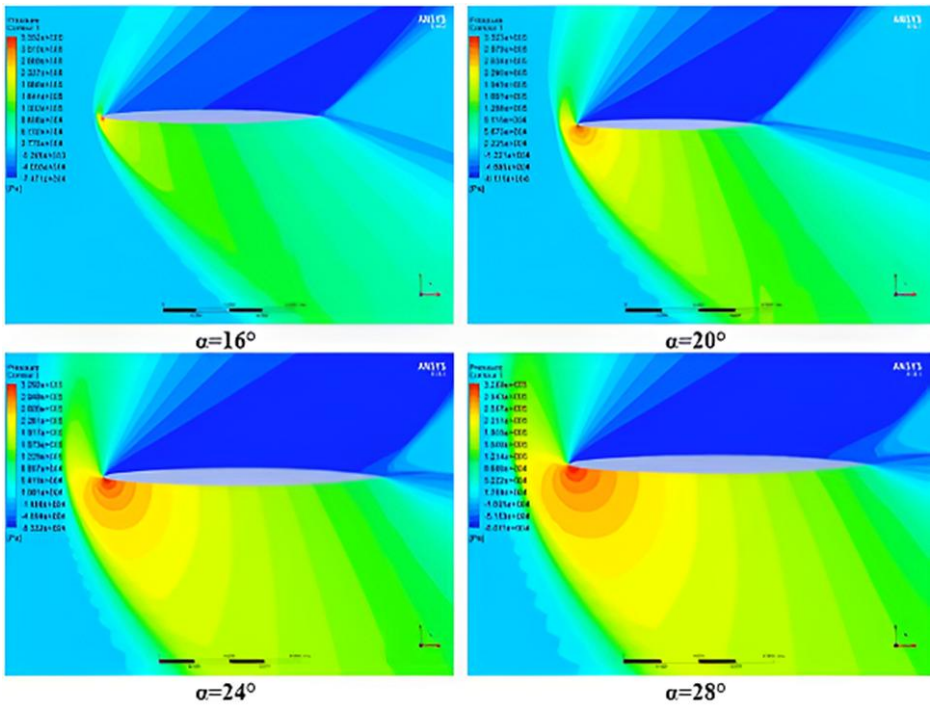

Fig 8: Pressure contours for Mach number 1.7.

Velocity Contours at Mach Number 1.7

The velocity contours for the current simulation are shown by figure 9 and 10. The red color in the velocity contours indicate higher velocity, while the green and yellow color indicate the moderate velocity. The low velocity is specified by the blue color. From the velocity contours, it is seen that, higher velocity is observed at the locations where the surface pressure is low. If the velocity contours are corelate with the pressure contours it can be seen that velocity is higher in the locations where the surface pressure is low. In opposite it can be said that velocity is lower where the surface pressure is higher. This correlation can be explained with the help of Bernoulli's theorem. Higher velocity is observed in the zone of silence. The flow separation point is identified by the blue colored region. The velocity in the lower surface of airfoil changes from higher magnitude to moderate magnitude with the increase of angle of attack. While the upper surface always subjected to higher velocity magnitudes.

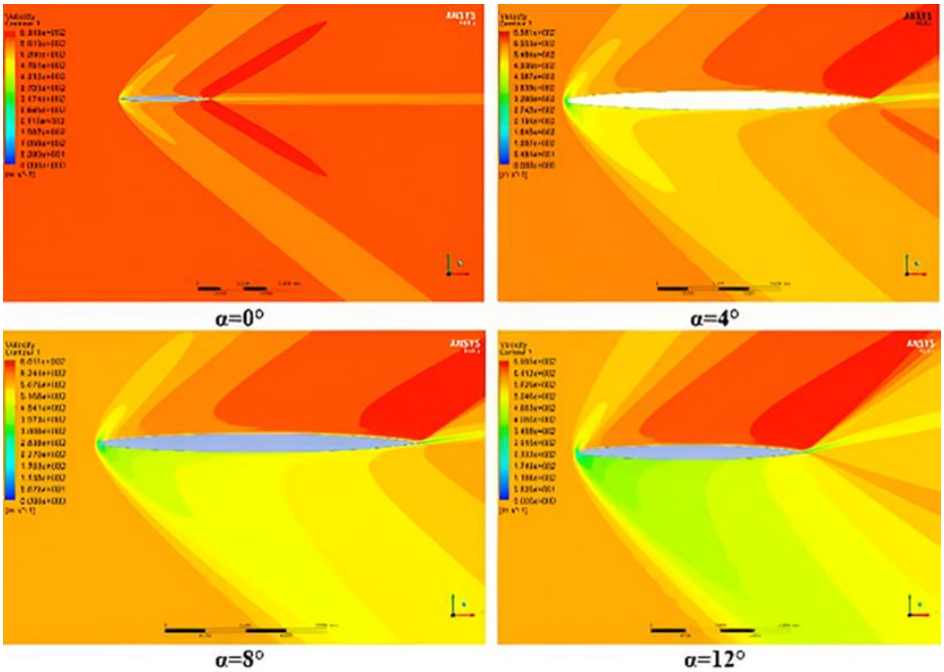

Fig 9: Velocity contours for Mach number 1.7.

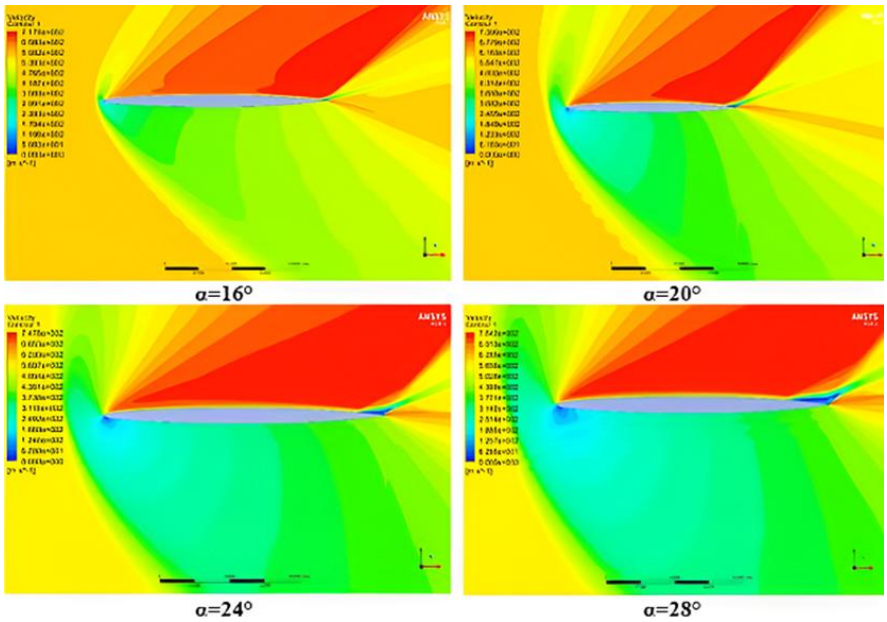

Fig 10: Velocity contours for Mach number 1.7.

V. Conclusion

This study investigated and visualized the flow chracteristics around a biconvex airfoil at a high Mach number supersonic flow. The investigation was done in a 2D flow field with the help of ANSYS Fluent using the SST k-ω turbulence model. The key findings are, with increase of angle of attack the lift and drag coefficient increases till stall occurs. After the stall these aerodynamic characteristics show undesired behavior. The biconvex airfoil under the simulation conditions, exhibits the maximum aerodynamic efficiency at 6° angle of attack. The flow separation point was also identified. The flow characteristics were visualized for different angle of attack. Mechanisms of surface pressure and velocity distribution were closely observed. To undestand the flow characteristics of a biconvex airfoil evidently and concisely, more investigations at different unique Mach numbers are recommended.

Abbreviations

Ma: Mach Number
C_L: Coefficient of Lift
C_D: Coefficient of Drag
C_L/C_D: Lift to Drag Ratio
α: Angle of Attack

Conflict of Interest

The authors declare that they do not have any conflict of interest.

Authors Contributions

D. Biswas: Conceptualization, methodology, formal analysis, data curation, writing original draft, visualization.
R. Mustak: Conceptualization, writing, review, editing, supervision.
S. Bakchi: Review, editing.

Corresponding Author: Rubiat Mustak, email: rubiat_kuet@me.kuet.ac.bd.

Acknowledgements

The authors gratefully acknowledge the support of the Department of Mechanical Engineering, Khulna University of Engineering and Technology, Khulna, Bangladesh, in completing this work successfully.

References

[1] J. D. Anderson, Fundamentals Of Aerodynamics, Fifth Edition In Si Units. New York: Mcgraw-Hill Education, 2011.
[2] E. L. Houghton And P. W. Carpenter, Aerodynamics For Engineering Students, 5. Ed., Reprinted. Amsterdam: Elsevier, Butterworth-Heinemann, 2008.
[3] S. Askari, M. H. Shojaeefard, And K. Goudarzi, "Numerical And Analytical Solution Of Compressible Flow Over Double Wedge And Biconvex Airfoils," Engineering Computations, Vol. 28, No. 4, Pp. 441–471, May 2011, Doi: 10.1108/02644401111131885.

[4] S. S. B. Bensiger And N. Prasanth, "Analysis Of Bi-Convex Airfoil Using Cfd Software At Supersonic And Hypersonic Speed," Elixir Mech. Engg, Vol. 53, Pp. 11695–11698, 2012.
[5] E. Kinaci, "Supersonic Flow Over A Double Circular Airfoil," Gas Dynamics Take Home Project 2013, Department Of Fluid Dynamics, University Of Duisburg Essen. Doi: 10.13140/Rg.2.1.4305.7125.
[6] Tejas Shivaji Tharkude And Dr. Zheng (Jeremy) Li, "Simulation Study Of Supersonic Natural Laminar Flow On Wing With Biconvex Airfoil," Ijert, Vol. 07, No. 03, Pp.366-373, 2018.
[7] C. Tulita, S. Raghunathan, And E. Benard, "Drag Reduction And Buffeting Alleviation In Transonic Periodic Flow Over Biconvex Airfoils," In 24th International Congress Of The Aeronautical Sciences, Yokohama, Japan, Sep. 2004.
[8] L. B. Schiff And J. L. Steger, "Numerical Simulation Of Steady Supersonic Viscous Flow," Aiaa Journal, Vol. 18, No. 12, Pp. 1421–1430, Dec. 1980, Doi: 10.2514/3.50902.
[9] L.-W. Chen, C.-Y. Xu, And X.-Y. Lu, "Numerical Investigation Of The Compressible Flow Past An Aerofoil," J. Fluid Mech., Vol. 643, Pp. 97–126, Jan. 2010, Doi: 10.1017/S0022112009991960.
[10] M. Saif Ullah Khalid And Afzaal M. Malik, "Modeling & Simulation Of Supersonic Flow Using Mccormack's Technique," In Proceedings Of The World Congress On Engineering 2009, London, U.K., Jul. 2009.
[11] Sarkar, S. And Mughal, S. B., "Cfd Analysis Of Effect Of Flow Over Naca 2412 Airfoil Through The Shear Stress Transport Turbulence Model," International Journal Of Mechanical And Production Engineering, Vol. 5, No. 7, 2017.
[12] R. K. Bansal, A Textbook Of Fluid Mechanics And Hydraulic Machines. New Delhi: Laxmi Publications, 2017.
[13] Mikhail Pavlovich Bulat And Pavel Victorovich Bulat, "Comparison Of Turbulence Models In The Calculation Of Supersonic Separated Flows," World Applied Sciences Journal, Vol. 27, No. 10, Pp. 1263–1266, 2013, Doi: 10.5829/Idosi.Wasj.2013.27.10.13715.
[14] E. Hosseini, "Cfd Analysis Of The Aerodynamic Characteristics Of Biconvex Airfoil At Compressible And High Mach Numbers Flow," Sn Appl. Sci., Vol. 1, No. 10, P. 1283, Oct. 2019, Doi: 10.1007/S42452-019-1334-2.